ON LOCALIZATION OF CARBON NANOTUBES IN WOVEN GLASS FIBER/EPOXY COMPOSITES AND ITS EFFECT ON TENSILE PROPERTIES

Larissa Gorbatikh[1], Alexander Haesch[2,3], Thijs Clarkson[2], Jan Ivens[1,2], Stepan V.Lomov[1], Ignaas Verpoest[1]

[1]*Katholieke Universiteit Leuven, Department of Metallurgy and Materials Engineering, Leuven, Belgium*
[2]*Department of Industrial Engineering, Lessius University College, Sint-Katelijne-Waver, Belgium*
[3] *Faculty of Materials Engineering, Georg Simon Ohm University of Applied Sciences, Nuremberg, Germany*
**email address of the corresponding author: Larissa.Gorbatikh@mtm.kuleuven.be*

Keywords: carbon nanotubes, dispersion, filtering, damage

Abstract
The dispersion of carbon nanotubes (CNTs) in epoxy resins that are to be used as a matrix material in fiber-reinforced composites is commonly targeted to be homogeneous and free of agglomerates. In the present paper we report experimental observations, showing that the uniform distribution of CNTs in fiber-reinforced composites is not necessarily a desired feature. The study was performed on a woven glass fiber composite produced using resin transfer moulding. Two different localization states of CNTs were achieved by choosing matrices with different dispersion qualities. For the resin with large agglomerates, CNTs tended to localize in the resin rich zones, while for the resin with smaller agglomerates, CNTs were somewhat homogeneously distributed in a composite. The CNT distribution/localization showed to influence the strain-to-failure of a composite and the density of transverse cracks. The composite with localized CNTs in the resin rich zones had a higher strain-to-failure (by 12%) and lower crack density (by 29%) in comparison with the virgin composite.

1 Introduction
The non-homogeneous distribution of CNTs in a composite on the meso-scale (for example, higher concentration of CNTs in resin rich zones combined with no CNTs inside fiber bundles) may have an important effect on composite mechanical properties. In particular, the onset and development of damage are expected to be affected by the CNT dispersion as they are directly linked to the meso-structure of a textile and the fiber distribution inside yearns. The goal of the present work is twofold: 1) to investigate positioning of CNTs in a woven glass fiber composite for two distinctly different CNTs dispersion states in the resin, and 2) to evaluate the effect of CNT localization on the composite tensile properties and damage development.

2 Materials and methods
2.1 Raw materials
The reinforcement is a woven roving E-glass fiber fabric EWR570-1270 from Taishan Fiberglass Inc. The resin system is Epikote 828LVEL combined with a 1,2-diaminocyclohexane hardener Dytek DCH-99 in a 100-15.2 weight ratio. The nano-scale

reinforcements are multi-wall carbon nanotubes (MWCNTs) from Nanocyl, which were supplied pre-dispersed in a bisphenol-A epoxy resin as a masterbatch (EpoCyl NC R128-02) at a high concentration.

2.2. CNT dispersion states

The dispersion state in this study is controlled through aging of the masterbatch. More specifically, two masterbatches are used: a freshly made (less than a month old) and aged (almost two years old) masterbatches. The masterbatches were stored on the shelf at room temperature. No particular storage conditions were enforced. Both systems have been prepared in the same fashion using the same type of components with the same quantities. Comparing results of the electrical impedance spectroscopy, it was found that the CNT-reinforced epoxy prepared from the aged masterbatch had a significantly higher specific conductivity (by five orders of magnitude) in comparison with the one made from the freshly made masterbatch. The diagrams of impedance vs. frequency revealed that the material from the aged masterbatch exhibited electrical percolation while this was not the case for the freshly made version, although both systems contained equal amounts of CNTs (0.3wt%). The backlight optical microscopy confirmed the presence of a network-like CNT structure for the aged system and a uniform distribution of small agglomerates in the system from the freshly prepared masterbatch. The two dispersion states are labeled here as a **U**niform state with small CNT **A**gglomerates (to be further referred to as the UA-case) and interconnected state where CNTs form a **N**etwork with larger features (to be referred to as the N-case). The largest CNT aggregates in the UA-case are on the order of 10μm. They are separated by agglomerates on the order of 1μm and smaller. In the N-case CNTs are formed into a network with pathways of ~25-50 μm in width and CNT-void areas in-between that are ~50-100 μm in size. The in-depth analysis of these two cases can be found in [1].

2.3 Production of composite plates.

Before composite production the CNT containing master batch is diluted with Epikote 828LVEL to obtain 0.3wt% of CNTs in epoxy. With the hardener added, the final concentration of CNTs in the resin is 0.26 wt%. Composite plates were produced using vacuum assisted resin transfer molding. Two types of plates were produced: 1) plates for mechanical testing, and 2) thin plates for backlight inspection and microscopy to characterize CNT position. Production parameters for the plates of the first type are listed in Table 1. The thin CNT doped plates for backlight inspection and microscopy were produced with a 1 mm spacer and contained only two plies of the glass fiber fabric. These plates had a fiber volume fraction of 45%. The production and characterization of thin plates (both for the UA-case and N-case studies) was done by the same operator. The post curing temperature was kept to 100°C for both cases.

Number of plies	7	Curing temperature	70°C
Spacer thickness	3.1 mm	Curing Pressure	4 bar
Degassing time	15 min	Curing time	1 hour at curing temperature
Injection temperature	40°C	Post Curing	150°C (N-case)
		Temperature	100°C (UA-case)
Injection Pressure	1 bar	Post Curing Time	2 hours at post curing temperature

Table 1. VARTM production parameters

2.4 Experimental methodology

2.4.1. Backlight inspection and microscopy

Thin plates were subjected to backlight inspection and microscopy to visualize filtration of CNTs. This idea was mainly inspired by the work in [2], where backlight inspection was used to examine CNT filtration on the level of a composite plate. In the present work we use the

same principle but on a smaller scale. Digital pictures were taken at two different magnifications to investigate filtration on the scale of a representative cell and at boundaries of individual yarns. In addition, several adjacent pictures were taken in a row and put together to create a 'stitched image'. This allowed a global view of a certain area with the benefit of high magnification of the individual pictures.

2.4.2 Tensile tests

The composite plates were cut into specimens 250 mm x 25 mm x 3 mm and equipped with glass fiber reinforced end tabs of 40 mm x 25 mm x 4 mm Tensile tests were done on Instron 4505 with a 100 kN load cell and hydraulic clamping jaws. All tensile tests were performed in the fiber direction and at a crosshead speed of 1 mm/min till specimen failure. For accurate strain measurement, an optical extensometer (digital image correlation system) was used. The surface of a specimen was captured with a camera every two seconds and images were then processed to obtain surface strains using LIMESS Messtechnik & Software GmbH set-up (Vic-3D, developed by Correlated Sollutions Inc.). The tests were also accompanied by registration of acoustic emission events using AMSY-5 system by Vallen Systems GmbH and two piezo-crystal sensors. A threshold value was set to 40dB. For analysis a curve with cumulative AE energy of events versus strain was used [3].

2.4.3. Damage characterization

Specimens were examined post-mortem using X-ray radiography. Before examination, samples are submerged in a bath of diiodomethane for four hours. The radiography was done using an X-TEK VTX160 device. Damage patterns were then studied in more detail with optical and/or scanning electron microscopy (SEM) on polished cross-sections. For the SEM examination samples were coated with a layer of gold and imaged with a Philips XL30 FEG microscope.

3. Results and discussion.

3.1 CNT localization in a composite

The area of a single representative cell (3x3 yarns) is examined in detail using backlight microscopy. The two images in Fig 1 are each composed out of about 100 individual images that were taken consecutively at a magnification of 240 times. Since glass is transparent, the white areas are attributed to the fiber yarns of both plies being aligned, while the dark crisscross lines represent the resin rich areas in between. The change in brightness indicates a difference in CNT concentration, caused by filtration of CNTs and CNT agglomerates during injection into the glass fibers. The white lines mark directions of the aligned glass fiber yarns. CNT agglomerates are clearly visible for the UA-case. Most of them can be found between yarns in resin rich zones and on the yarn boundaries. Many of the smaller agglomerates also managed to get inside the yarns and are situated in-between fibers. Nevertheless, CNT concentration inside the yarns is lower. Hence a local filtering effect on the yarn boundaries can be identified, hindering large CNT agglomerates to penetrate the yarns and thus lowering CNT concentration around individual glass fibers inside the fiber bundles. A similar examination is done for the N-case, but positioning of CNTs is found to be quite different there. While some CNT agglomerates can be identified at the yarn boundaries, there seem to be a lot less of them or not at all inside the yarns. In addition, resin rich zones appear a lot darker, indicating a larger CNT concentration there. Thus, the local filtering effect on the yarn boundaries is more pronounced in the N-case.

To conclude, the textile structure filters nanotube agglomerates above a certain size during the RTM process. Due to the dense packing of glass fibers inside fiber yarns, the yarn boundaries act as barriers for CNT agglomerates. This leaves only a small fraction of CNTs being able to penetrate the yarns and situate themselves around individual fibers. The majority

of carbon nanotubes are left behind in the resin rich zones with no contact to the primary reinforcement structure.

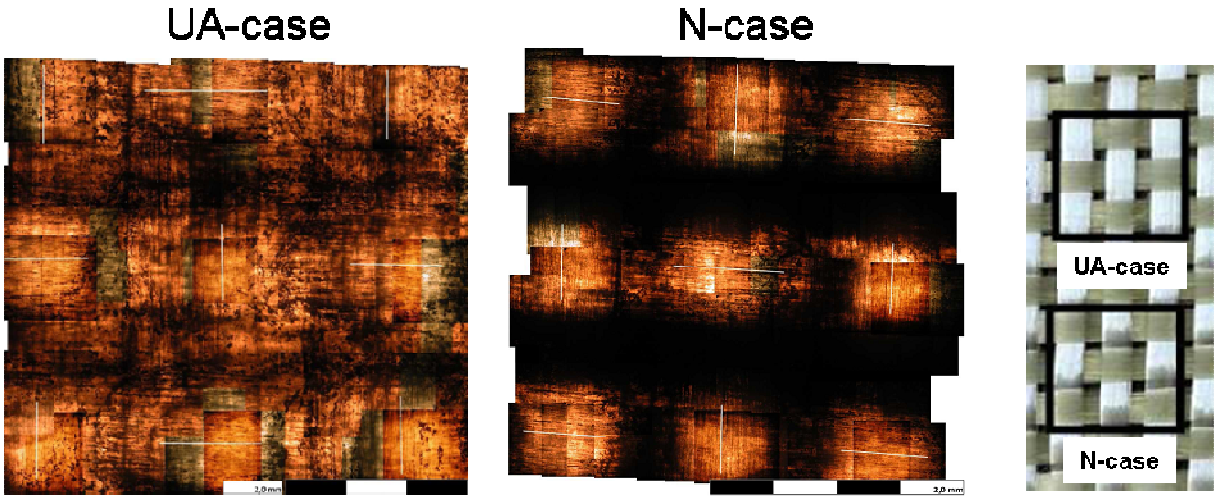

Figure 1 Backlight microscopy images of (a) one representative cell of the glass fiber fabric for two dispersion states; (b) a close up on the resin rich areas for the same dispersion states.

3.2. Tensile test results

Table 2 gives overview of tensile properties for the UA-case. The Young's modulus and tensile strength are also normalized to Vf = 50%. The normalization is done for each individual specimen and the average is taken over the number of specimens tested for the specific property. It can be seen that CNTs in the matrix have no influence on the Young's modulus of the composite. The strength is also not affected by the presence of CNTs in the present case. The only affected property is the strain to failure, which is decreased by 12.2%. The observed decrease in this property is statistically significant with the confidence level of 100%.

The accumulated energy of AE events recorded during tensile tests are plotted over strain for all specimens. These plots are used to extract characteristic damage development thresholds ε_{min}, ε_1, and ε_2 ([3]) that are also listed in Table 2. There is a clear shift of damage development thresholds to higher strains, indicating a delay of damage initiation and damage propagation in the system reinforced with CNTs. While ε_{min}, which is related to the first ad hoc appearance of microcracks (usually connecting a few fibers), is shifted only by +5%, ε_1 and ε_2 are both significantly increased. Hence the onset of transverse cracks and further damage development occur with a delay in comparison with the reference material, by 31.4% and 25.0%, respectively. Since transverse cracks are formed inside fiber bundles, the shift of ε_1 indicates that CNTs are managed to get inside yarns. This is in agreement with the observations from backlight microscopy reported above.

The data for the N–case were processed the same way as for the UA-case study and presented in Table 3. The addition of CNTs does not affect the Young's modulus and strength of the glass fiber composites. The strain-to-failure, on the other hand, is increased in the presence of CNTs by 10.4% with the confidence level of 99%. From the cumulative AE energy curves it is found that the addition of CNTs in the matrix with the N-dispersion has no apparent effect on the acoustic emission events. There is no statistical difference in ε_1 and ε_2 for the CNT containing and the reference composites. These results are somewhat expected as for of the network-like CNT structure CNTs localized in resin rich zones without getting inside fiber bundles. Since transverse cracks are formed inside fiber bundles and CNTs are not there, no change for the onset of transverse cracks is expected. Thus, the AE data indirectly confirm that CNTs remain outside of fiber bundles.

		Thickness, mm		V_f, %	E, GPa		Strength, MPa		Strain to failure, %		ε min		ε 1		ε 2	
		Average	St. dev		Average	St dev	Average	St dev	Average	St dev	Average	St dev	Average	St dev	Average	St dev
Reference composite	As measured	3.23	0,03	48.4	25.1	0.5	495.09	15.9	2.94	0.16	0.23	0.09	0.26	0.04	0.36	0.06
	Normalized			50	25.9		511.6	17.9								
Number of specimens		8		8	8		8		8		8		6		8	
CNT-reinforced composite	As measured	3.26	0,01	48	25.8	0.2	468.67	23.5	2.58	0.13	0.24	0.09	0.34	0.07	0.45	0.07
	Normalized			50	26.9		488.4	24.3								
Number of specimens		8		8	8		8		8		8		8		8	
Relative difference, %					3.9		-4.5		-12.2		4.3		30.8		25.0	
Confidence level, %							97.7		100.0		58.6		98.7		99.3	

Table 2. Tensile test results for the glass fiber composites in the UA-case study.

		Thickness, mm		V_f, %	E, GPa		Strength, MPa		Strain to failure,		ε min		ε1		ε2	
		Average	Std dev		Average	Std dev	Average	Std dev	Averag	Stddev	Average	Std dev	Average	Std dev	Average	Std dev
Reference composite	As measured	3.21	0.05	49.5	26.6	0.6	451.5	8.3	2.49	0.12	0.23	0.03	0.28	0.05	0.52	0.05
	Normalized			50	26.7	0.7	453	8.8								
Number of specimens					4		4		4		4		4		4	
CNT-reinforced composite	As measured	3.13	0.05	50.8	25.6	2.3	487.7	13.7	2.75	0.09	0.17	0.03	0.26	0.03	0.51	0.03
	Normalized			50	25	2.7	474.6	18.4								
Number of specimens					3		3		3		3		3		3	
Relative difference,					-6.4		4.8		10.4		-26.1		-7.1		-1.9	
Confidence level, %					87.0		96.0		99.0		98.0		71.7		61.4	

Table 3. Tensile test results for the glass fiber composites in the N-case study.

3.3 Damage characterization

In the UA-study the density of transverse cracks was estimated using two approaches: 1) from the surface of tested specimens and 2) from polished cross-sections of tested specimens. Cracks were counted on specimens of 25 mm x 25 mm that were cut out from failed specimens more than 1 cm away from the failure plane. The examined areas included four representative cells and each representative cell included five locations on transverse yarns that were cracked. Only distinct cracks were counted when calculating the cracks density per visible part of a yarn. The average number of distinct cracks per yarn is decreased in the composite with CNTs by 11.36%. After that the crack density was calculated per cm length of a specimen (Table 4). No apparent difference was found in crack densities counted from polished cross sections (Table 4). Transverse cracks in the CNT-reinforced composite, however, looked somewhat different than the same cracks in the reference material. They were less straight and often changed trajectory in places where there was no obvious reason for it. This can be understood if one imagines that the matrix has a heterogeneous structure. Indeed, CNT agglomerates are expected to change crack paths upon approach, as cracks are likely to go around the CNT agglomerates following higher stress concentrations than to enter them.

	Density of surface cracks, cracks/cm				Density of cracks through thickness, cracks/cm		
	Number of specimens	Number of cells	average	std dev	Number of specimens	average	std dev
Reference GFRP	7	27	11.9	2.0	9	15.4	3.5
CNT-reinf. composite	7	28	10.5	2.4	10	16.5	5.7
Relative difference, %			-11.8			+7	
Confidence level. %			98.8			68.8	

Table 4 Density of transverse cracks in the UA-case study.

For the N-study, damage in the composite is characterized with X-ray radiography. The images are taken from specimens tested till failure. Table 5 offers statistically processed data of these images. The images present a very homogenous distribution of transverse cracks along the length of the sample. The scatter is induced by the fact that there are more cracks near the edges of the samples than in the centre. An overall reduction of 29% is noted for the CNT reinforced samples and shown to be statistically significant.

	Number of processed			Crack density, cracks/cm^2	
	specimens	images	squares	average	std dev
Reference GFRP	3	12	183	15.8	4.2
CNT-reinforced GFRP	3	12	150	11.2	2.2
Relative difference, %				-29	
Confidence level, %				99.9	

Table 5 Density of transverse cracks in the N-study (X-ray radiography).

4 Conclusions

In the course of the work the following conclusions have been made:

- Backlight inspection and microscopy revealed a filtering effect of CNTs on the scale of the fabric architecture. This effect is attributed to the difference in the original dispersion state in the resin. For the case of small isolated CNT agglomerates, CNTs are able to enter fiber bundles. This conclusion is also supported by the AE measurements, which indicate a

shift in damage development thresholds towards higher strains. For the state of dispersion where CNTs form a network with large features, it is found that CNTs tend to localize in resin rich zones without entering fiber bundles. The AE registration data are consistent with this observation as no change in the onset of transverse cracks is recorded.

- The presence of CNTs in a composite has no effect on the Young's modulus, only minor effect on the strength, and somewhat significant effect on the strain-to-failure. The composite with CNTs in the resin rich zones has a higher strain-to-failure and lower density of transverse cracks in comparison with a virgin composite. In the meantime, a somewhat lower strain-to-failure and about the same crack density are measured for the composite where CNTs are clustered in small individual agglomerates.

Acknowledgements

The work at KU Leuven was performed in the scope of the GOA/10/004 project "New model-based concepts for nano-engineered polymer composites", funded by the Research Council of KU Leuven. The CNT containing masterbatch was received from Nanocyl S.A in the framework agreement between the Department of Metallurgy and Materials Engineering, KU Leuven and Nanocyl S.A.. We thank Nakul Prasad for characterization of surface cracks and MohammadAli Aravand for optical microscopy images in Fig.1. The help of technicians Bart Pelgrims, Kris Van de Staey and Manuel Adams is also gratefully acknowledged.

References

[1] Aravand A., Gorbatikh L., Lomov S.V., Verpoest I., Evolution of carbon nanotube dispersion in preparation of a fiber-reinforced epoxy-based composite: from a CNT masterbatch to a composite, Proceeding of *the 15th European Conference on Composite Materials* (ECCM 15), Venice, Italy, June 24-28 (2012).

[2] Rieber, G., Grieser T., Grad P., Mitschang P., Processing and evaluating CNT doped laminates, Proceeding of *the SAMPE 2011*. Society for the Advancement of Material and Process Engineering, Long Beach, California 23-26 May (2011).

[3] Lomov SV, Ivanov DS, Truong TC, Verpoest I, Baudry F, Vanden Bosche K, Xie H. Experimental methodology of study of damage initiation and development in textile composites in uniaxial tensile test. *Composite Science and Technology*; **68**, pp. 2340-2349 (2008).